

Use of Taylor Series Expansions for Time Savings in Computation of Accurate Transducer Pressure Fields

ERNEST L. MADSEN, TIMOTHY J. HALL, JAMES A. ZAGZEBSKI,
AND MICHAEL F. INSANA, MEMBER, IEEE

Abstract—In the method of data reduction used in our laboratory to determine acoustic backscatter coefficients in tissues and tissue-like media, computation of the complex acoustic pressure in an attenuating medium due to a nonfocused disk radiator is required at a large number of field points and over a frequency band of about 1 MHz. Computer CPU time and input/output time can be considerable because of the need to evaluate an integral corresponding to each field point P and frequency, ω . The fact that the frequency dependence of this integral is restricted to a factor in the integrand of the form $\exp(ikr')$, where r' is the dummy variable and $k \equiv k(\omega)$ is the complex wave number, makes the integral part of the expansion in a Taylor series straightforward. The first five terms of the Taylor series have been derived, and tests of the accuracy of the expansion are presented. While maintaining adequate accuracy, the CPU time savings accrued through use of the series corresponds to a factor of 1/7 and an input/output time savings factor of at least 1/6. (The factor 1/7 means, e.g., that a CPU time of 35 min without using the Taylor series becomes 5 min using the Taylor series.)

I. INTRODUCTION

CONSIDERABLE WORK in our laboratory requires computation of the pressure field of a focused transducer or disk transducer for pulsed emissions. When the (linear) Helmholtz equation applies, such pressure fields can be expressed in the form of linear superpositions of sinusoidally varying continuous wave beams spanning some range of frequencies [1]. The continuous wavebeams can be computed by assuming the source to be composed of a uniformly distributed set of equivalent monopole sources oscillating sinusoidally in time and all having the same phase; the uniform distribution means that the number of monopole sources per unit area over the active element of the transducer surface is constant, and this is true no matter how small an area element is considered.

Determination of the sinusoidally varying pressure at any point \vec{r} in the field of the transducer for some frequency ω requires computing the integral

$$A_0(\vec{r}, \omega) = \iint_S \frac{e^{ik|\vec{r}-\vec{r}''|}}{|\vec{r}-\vec{r}''|} ds'' \quad (1)$$

Manuscript received April 24, 1986; revised August 24, 1986. This work was supported in part by the National Institutes of Health under Grants R01 CA25634 and R01 CA39224.

E. L. Madsen, T. J. Hall, and J. A. Zagzebski are with the Department of Medical Physics, 1530 Medical Science Center, University of Wisconsin, Madison, WI 53706, USA.

M. F. Insana is with the Center for Devices and Radiological Health, Food and Drug Administration, Rockville, MD 20857, USA.

IEEE Log Number 8612684.

where ds'' is the area element at position \vec{r}'' on the transducer surface and S is the total radiating surface of the transducer.

The double integral form for $A_0(\vec{r}, \omega)$ can be reduced to nonintegral form only on the axis of symmetry of the transducer [2]. Off axis, the double integral can be reduced to the sum of a single integral and a nonintegral term, and this sum containing the single integral has been shown to be accurate by direct comparison with experiment for the case of a spherical shell-type focused transducer [1]. $A_0(\vec{r}, \omega)$ takes the form

$$A_0(\vec{r}, \omega) = \frac{2A}{ks} \left[\int_C^D \beta(u) e^{iu} du - iF \right] \quad (2)$$

where A is the radius of curvature of the radiating surface and s is the distance from the center of curvature of the radiating element to the field point at \vec{r} . Also, k is the wavenumber, and C/k and D/k depend on the geometry of the radiating element only and not on k or ω . That the single integral version of $A_0(\vec{r}, \omega)$ has the above form can be seen by referring to [1, pp. 1509, 1511]. The quantities F , C , D , and $\beta(u)$ are also given in that reference.

Equation (2) applies for focused radiators and can be extended to nonfocused radiators by taking the limit $A \rightarrow \infty$. (Note that $A \rightarrow \infty$ means that $A/s \rightarrow 1$ for field points at finite distances from the radiator.) The result of the latter limiting operation is

$$A_{0N}(\vec{r}, \omega) = \frac{2}{k} \left[\int_C^D \beta(u) e^{iu} du - iF \right] \quad (3)$$

where C , D , $\beta(u)$, and F have the limiting forms ($A \rightarrow \infty$):

$$C = k[(a-x)^2 + y^2]^{1/2}$$

$$D = k[(a+x)^2 + y^2]^{1/2}$$

$$\beta(u) = \cos^{-1} \left[\frac{-a^2 + (u/k)^2 + x^2 - y^2}{2x[(u/k)^2 - y^2]^{1/2}} \right] \quad (4)$$

and

$$F = \begin{cases} \pi[e^{iC} - e^{iD}], & x \leq a \\ 0, & x \geq a \end{cases} \quad (5)$$

The quantities y and x are (positive) distances as shown in Fig. 1. y is the distance from the field point (at which

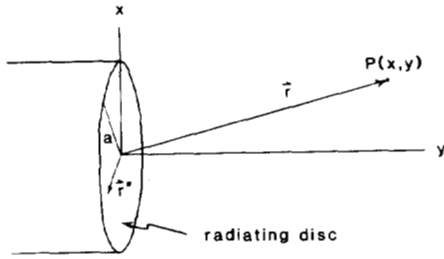


Fig. 1. Diagram of planar circular disk transducer modeled. Radius of disk is a , origin of coordinate system is taken to be at center of radiating disk, and y axis is perpendicular to disk. Position vector \vec{r} extends from origin to field point $P(x, y)$. Position vector \vec{r}' extends from origin to arbitrary point on radiating surface.

the pressure is to be found) to the plane containing the radiating disk, and x is the distance from the field point to the axis of symmetry of the transducer. As can be seen in Fig. 1, $r \equiv |\vec{r}| = (x^2 + y^2)^{1/2}$ is the distance from the center of the disk radiator to the field point. These expressions are equivalent to those derived by Lockwood and Willette [3] for a nonfocused disk radiator.

When evaluation of some function of $A_0(\vec{r}, \omega)$ over ranges of ω and/or \vec{r} is required, considerable computer time can be involved because, for each combination of \vec{r} and ω , a single numerical integration must be done. For example, in our laboratory a data reduction method is in use for accurate determination of acoustic backscatter coefficients [4], [5]. This method typically requires computation of $A_0(\vec{r}, \omega)$ at about 31 frequencies for each field point \vec{r} within the volume of interest. Equations (13), (15), and (17) of [4] particularize the involvement of $A_0(\vec{r}, \omega)$ over a band of frequencies. Much more demanding of computer time is the computer generation of B -scan texture patterns [6], [7]; because of the broad-band nature of clinical type pulsers, $A_0(\vec{r}, \omega)$ typically must be evaluated at about 100 frequencies for each field point \vec{r} . (See [7, eq. (8)] for the involvement of $A_0(\vec{r}, \omega)$ over a range of frequencies.) One way to reduce considerably the computer time needed, while still maintaining accuracy, is to introduce Taylor series expansions. In this paper the Taylor series expansion in frequency is developed for the case of the nonfocused transducer. Accurate expansion coefficients through four terms are developed as well as a good approximation of the fifth coefficient. Tests of the accuracy of the expansions by comparison with correct results, obtained using numerical integration via Gaussian quadrature, are also presented.

II. DEVELOPMENT OF THE TAYLOR SERIES EXPANSION IN FREQUENCY

It is desired to approximate $A_{0N}(\vec{r}, \omega)$ in the neighborhood of some frequency ω_0 , using a Taylor series expansion in ω . Rewriting (3) with a change of variables of integration given by $r' = u/k$, we have

$$A_{0N}(\vec{r}, \omega) = 2 \int_{C'}^{D'} \gamma(r') e^{ikr'} dr' - \frac{2iF}{k} \quad (6)$$

where $k = k(\omega)$ contains all of the dependence of

$A_{0N}(\vec{r}, \omega)$ on ω . Note that, if the beam exists in an attenuating medium, then $k(\omega) = \omega/c(\omega) + i\alpha(\omega)$, where $\alpha(\omega)$ is the frequency-dependent attenuation coefficient and $c(\omega)$ is the—perhaps frequency-dependent—ultrasonic speed in the medium. The limits on the integral and $\gamma(r')$ are independent of ω :

$$\begin{aligned} D' &= D/k = [(a+x)^2 + y^2]^{1/2} \\ C' &= D/k = [(a-x)^2 + y^2]^{1/2} \\ \gamma(r') &= \cos^{-1} \left[\frac{-a^2 + r'^2 + x^2 - y^2}{2x(r'^2 - y^2)^{1/2}} \right]. \end{aligned} \quad (7)$$

F is a function of ω through k , however.

To reduce the very large phases involved on the right side of (6) (viz., kr' of the integrand), it is desirable to expand the quantity $e^{-ikr} A_{0N}(\vec{r}, \omega)$ instead of $A_{0N}(\vec{r}, \omega)$. Minimizing these phases can avoid related numerical computation errors. We have

$$e^{-ikr} A_{0N}(\vec{r}, \omega) = 2 \int_{C'}^{D'} \gamma(r') e^{ik(r'-r)} dr' - \frac{2iF e^{-ikr}}{k} \quad (8)$$

where $k|r'-r| \ll kr'$, and, in F ,

$$\left| k[(a-x)^2 + y^2]^{1/2} - kr \right| \ll k[(a-x)^2 + y^2]^{1/2}$$

and $k|y-r| \ll kr$ for r sufficiently large.

The needed derivatives of $e^{-ikr} A_{0N}(\vec{r}, \omega)$ with respect to ω are conveniently done by using the chain rule, viz., applying

$$\frac{d}{d\omega} = \frac{dk}{d\omega} \frac{d}{dk}$$

to $A_{0N}(\vec{r}, \omega)$ as many times as required. Expanding about $\omega = \omega_0$, the first term in the series is, of course, $e^{-ik_0 r} A_{0N}(\vec{r}, \omega_0)$ where $k_0 \equiv \omega_0/c(\omega_0) + i\alpha(\omega_0)$. The second term has the form

$$\frac{d}{d\omega} [e^{-ikr} A_{0N}(\vec{r}, \omega)] \Big|_{\omega=\omega_0} \cdot (\omega - \omega_0)$$

and the third term,

$$\frac{1}{2!} \frac{d^2}{d\omega^2} [e^{-ikr} A_{0N}(\vec{r}, \omega)] \Big|_{\omega=\omega_0} \cdot (\omega - \omega_0)^2,$$

etc.

The chain rule introduces various orders of derivatives of k with respect to ω . To reduce the complexity of the resulting Taylor series expansion with little (if any) loss in accuracy, we assumed that $c(\omega)$ is a constant and used the fact that experimental measurements of $\alpha(\omega)$ can be very well approximated by a quadratic curve fit of the form $\alpha(\omega) = \alpha_0 + \alpha_1\omega + \alpha_2\omega^2$ [8].¹ Thus

¹If the frequency dependence of the ultrasonic speed $c(\omega)$ is considered important, then the real part of the complex wave number, $\omega/c(\omega)$, can be written as a quadratic function of ω where the coefficients are determined experimentally or by application of the Kramers-Kronig relations.

$$\frac{d^n k(\omega)}{d\omega^n} = 0, \quad \text{for } n \geq 3.$$

For notational convenience we define the Taylor series coefficients to be

$$\begin{aligned} a_0 &\equiv e^{-ik_0 r} A_{0N}(\vec{r}, \omega_0), \\ a_1 &\equiv \frac{1}{1!} \frac{d}{d\omega} [e^{-ikr} A_{0N}(\vec{r}, \omega)] \Big|_{\omega=\omega_0} \\ &\vdots \\ a_n &\equiv \frac{1}{n!} \frac{d^n}{d\omega^n} [e^{-ikr} A_{0N}(\vec{r}, \omega)] \Big|_{\omega=\omega_0} \\ &\vdots \end{aligned}$$

Then the Taylor series in ω takes the simple form

$$\begin{aligned} e^{-ikr} A_{0N}(\vec{r}, \omega) &= a_0 + a_1(\omega - \omega_0) \\ &\quad + a_2(\omega - \omega_0)^2 + \dots \\ &\quad + a_n(\omega - \omega_0)^n + \dots \end{aligned}$$

We have determined the exact forms for $a_0, a_1, a_2,$ and a_3 . Coefficient a_4 has been approximated by including the contribution from the integral term in (6) and neglecting the nonintegral term $2iF/k$. This means that a_4 is accurate for $x \geq a$ since $F = 0$ in that region, but the accuracy is compromised for $x < a$. In the tests below, it will be seen that dropping the dependence of a_4 on F for $x < a$ is justified in most cases. This particular approximation is desirable since the n th derivative of the integral term is very easily determined. This is because

$$\begin{aligned} \frac{d^n}{dk^n} \left[2 \int_{C'}^{D'} \gamma(r') e^{ik(r'-r)} dr' \right] \\ = 2 \int_{C'}^{D'} \gamma(r') [i(r'-r)]^n e^{ik(r'-r)} dr' \end{aligned}$$

and, with the quadratic approximation for $k(\omega) = \omega/c + i\alpha(\omega)$,

$$\begin{aligned} \frac{d^4}{d\omega^4} &= 3 \left[\frac{d^2 k}{d\omega^2} \right]^2 \frac{d^2}{dk^2} + 6 \left[\frac{dk}{d\omega} \right]^2 \frac{d^2 k}{d\omega^2} \frac{d^3}{dk^3} \\ &\quad + \left[\frac{dk}{d\omega} \right]^4 \frac{d^4}{dk^4}, \end{aligned}$$

we have

$$\begin{aligned} a_4 &= \frac{2}{4!} \left[\frac{d^4}{dk^4} 2 \int_{C'}^{D'} \gamma(r') e^{ik(r'-r)} dr' \right]_{\omega=\omega_0} \\ &= \frac{1}{12} \int_{C'}^{D'} \gamma(r') \left\{ 3 \left[\frac{d^2 k}{d\omega^2} \right]^2 [i(r'-r)]^2 \right. \\ &\quad + 6 \left[\frac{dk}{d\omega} \right]^2 \left[\frac{d^2 k}{d\omega^2} \right] [i(r'-r)]^3 \\ &\quad \left. + \left[\frac{dk}{d\omega} \right]^4 [i(r'-r)]^4 \right\}_{\omega=\omega_0} e^{ik_0(r'-r)} dr'. \end{aligned}$$

The other series coefficients are

$$\begin{aligned} a_0 &= e^{-ik_0 r} A_{0N}(\vec{r}, \omega_0) \\ a_1 &= \left[\frac{dk}{d\omega} \right]_{\omega=\omega_0} \left\{ 2i \int_{C'}^{D'} \gamma(r') (r'-r) e^{ik(r'-r)} dr' \right. \\ &\quad \left. + (b/k^2) [(k\delta - 1) e^{\delta k} + (1 - kd) e^{kd}] \right\}_{\omega=\omega_0} \\ a_2 &= \frac{1}{2} \left\{ 2 \int_{C'}^{D'} \gamma(r') \left[i \frac{d^2 k}{d\omega^2} (r'-r) \right. \right. \\ &\quad - \left[\frac{dk}{d\omega} \right]^2 (r'-r)^2 \left. \right] e^{ik(r'-r)} dr' \\ &\quad + b e^{k\delta} \left[\frac{d^2 k}{d\omega^2} k^{-2} (\delta k - 1) + \left[\frac{dk}{d\omega} \right]^2 k^{-3} (2 - 2\delta k) \right. \\ &\quad \left. + \delta^2 k^2 \right] + b e^{kd} \left[\frac{d^2 k}{d\omega^2} k^{-2} (1 - kd) \right. \\ &\quad \left. + \left[\frac{dk}{d\omega} \right]^2 k^{-3} (-2 + 2kd - k^2 d^2) \right] \Big\}_{\omega=\omega_0}, \\ a_3 &= \frac{1}{6} \left\{ 2 \int_{C'}^{D'} \gamma(r') \left[-3 \frac{dk}{d\omega} \frac{d^2 k}{d\omega^2} (r'-r)^2 \right. \right. \\ &\quad - i \left[\frac{dk}{d\omega} \right]^3 (r'-r)^3 \left. \right] e^{ik(r'-r)} dr' \\ &\quad + b e^{k\delta} \left[\left[\frac{dk}{d\omega} \right]^3 (-6k^{-4} + 6\delta k^{-3} - 3\delta^2 k^{-2} + \delta^3 k^{-1}) \right. \\ &\quad + 3 \left[\frac{dk}{d\omega} \right] \left[\frac{d^2 k}{d\omega^2} \right] (2k^{-3} - 2\delta k^{-2} + \delta^2 k^{-1}) \left. \right] \\ &\quad - b e^{kd} \left[\left[\frac{dk}{d\omega} \right]^3 (-6k^{-4} + 6dk^{-3} - 3d^2 k^{-2} + d^3 k^{-1}) \right. \\ &\quad \left. + 3 \left[\frac{dk}{d\omega} \right] \left[\frac{d^2 k}{d\omega^2} \right] (2k^{-3} - 2dk^{-2} + d^2 k^{-1}) \right] \Big\}_{\omega=\omega_0} \end{aligned}$$

where $\delta \equiv i \{ [(a-x)^2 + y^2]^{1/2} - r \}$, $d \equiv i(y-r)$, and

$$b = \begin{cases} -2\pi i, & \text{if } x \leq a \\ 0, & \text{if } x > a \end{cases}$$

III. ACCURACY TESTS

Nonfocused transducers having a diameter of 12.7 mm have been used in our data acquisition for determination of backscatter coefficients of tissues and tissuelike materials. Tests of the accuracy of the (truncated) Taylor series are reported here for typical experimental conditions involved in these measurements. The transducer modeled has a diameter of 12.7 mm, and the reference frequency is $\omega_0 = 3.0 \text{ MHz} = 6\pi \times 10^6 \text{ rad/s}$.

The results are shown in Figs. 2-8. The solid lines correspond to correct computations in which the integration in (8) is performed numerically via Gaussian quadrature.

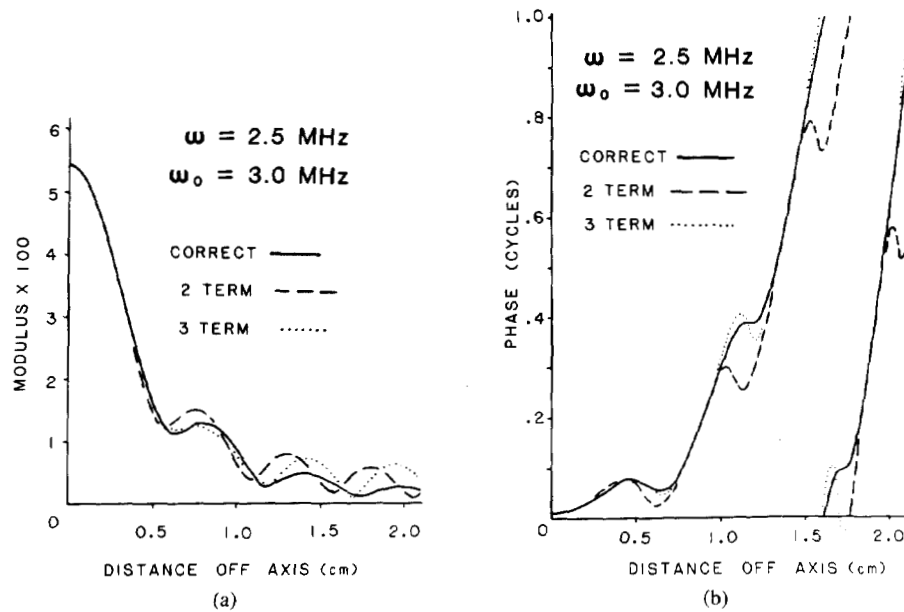


Fig. 2. Graphs showing increase in accuracy of Taylor series as number of terms kept increases from 2 (dashed lines) to 3 (dotted lines). (a) Modulus. (b) Phase. Frequency at which computations were made is 2.5 MHz, and reference frequency is 3.0 MHz. Axial distance y is fixed at 11.0 cm, distal 4.0 cm of which contains attenuating tissue-mimicking material. Correct curves, obtained by direct numerical integration, are solid lines.

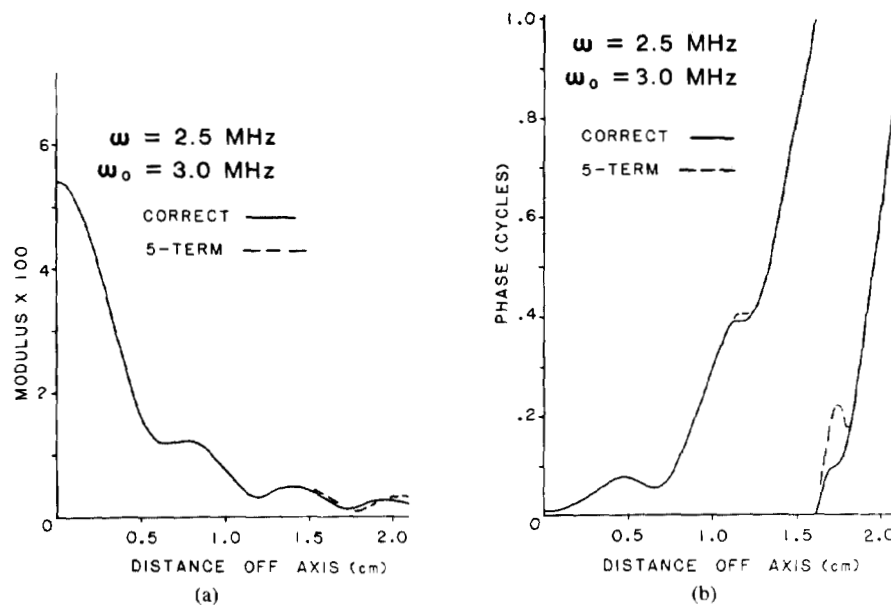


Fig. 3. Graphs showing five-term Taylor series results (dashed lines) for modulus (a) and phase (b) of $A_{0N}(\vec{r}, \omega)$ compared with correct results (solid lines). All other conditions correspond to those of Fig. 2.

Dashed and dotted curves correspond to calculations using Taylor series. In each figure part (a) shows the modulus of $A_{0N}(\vec{r}, \omega)$ and part (b) shows its phase. Also, in all figures the abscissa is x , the distance off-axis for a fixed value of y ; such plots are commonly referred to as lateral beam profiles.

In Figs. 2-6, y is 11.0 cm, and the 4.0-cm section of y furthest from the transducer exists in tissuelike material

having an ultrasonic speed of 1580 m/s and an attenuation coefficient of $\alpha(\omega) = 0.245 \text{ dB} \cdot \text{cm}^{-1} + 0.297 \text{ dB} \cdot \text{cm}^{-1} \text{ MHz}^{-1} \omega + 0.0391 \text{ dB} \cdot \text{cm}^{-1} \text{ MHz}^{-2} \omega^2$.² The remaining 7.0 cm of the 11.0 cm distance y consists of water. Appropriate equivalent values of c and α were used

²The values of c and the curve-fitted coefficients in $\alpha(\omega)$ resulted from measurements on an actual test sample of tissue-mimicking material.

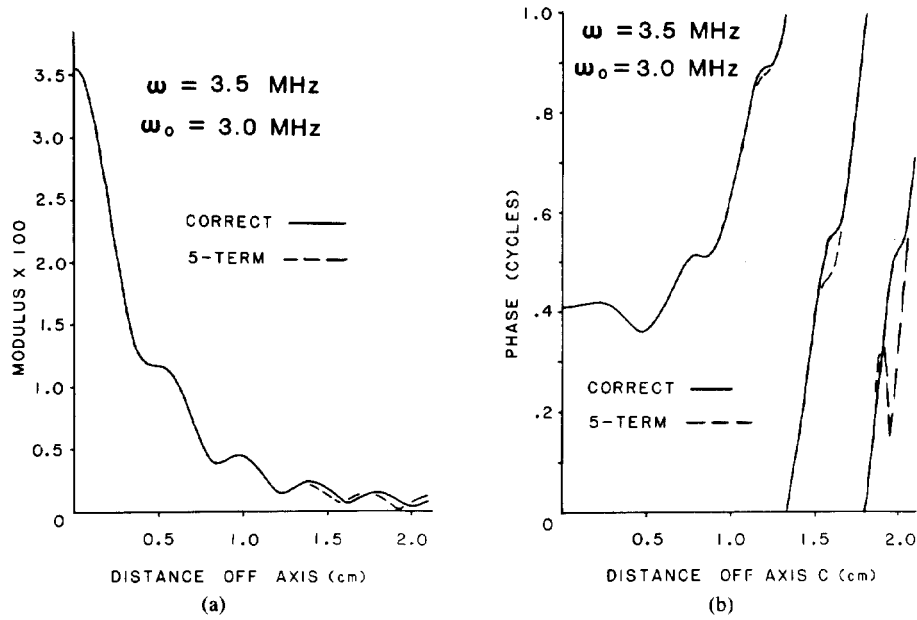


Fig. 4. Five-term Taylor series results (dashed lines) compared with correct results (solid lines) for frequency of 3.5 MHz. All other conditions correspond to those of Fig. 2.

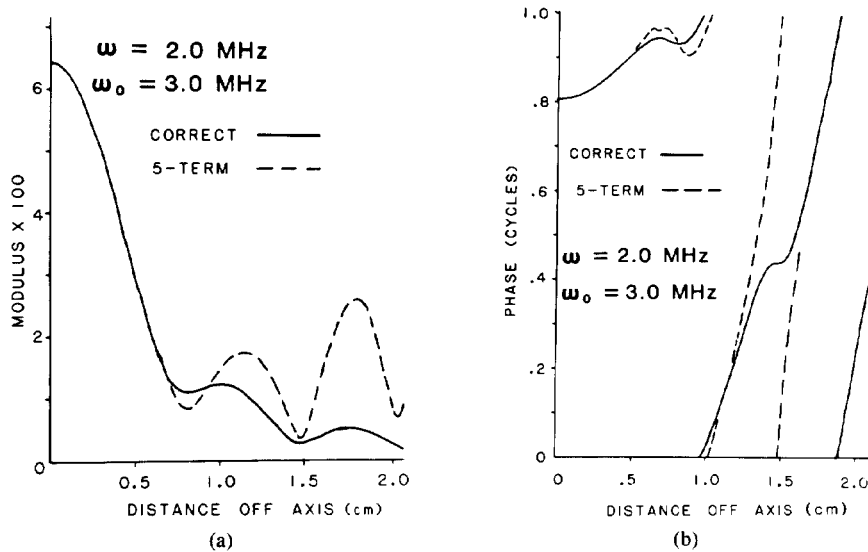


Fig. 5. Five-term Taylor series results (dashed lines) compared with correct results (solid lines) for frequency of 2.0 MHz. All other conditions correspond to those of Fig. 2.

to compute the complex wavenumber $k(\omega)$ used in all computations.

Figs. 2 and 3 illustrate the improvement in the approximation as the number of terms kept in the Taylor series increases from two to three to five. The frequency represented is 2.5 MHz. Inclusion of all five terms yields excellent accuracy for both amplitude and phase even through the second side lobe. All remaining figures correspond to the inclusion of all five terms of the Taylor series.

Fig. 4 corresponds to a frequency of 3.5 MHz. Again,

inclusion of all five terms yields excellent agreement between the Taylor series result and the correct calculation.

When the difference between the frequency of interest ω and the 3.0-MHz reference frequency reaches 1 MHz, the degree of accuracy degenerates considerably beyond an off-axis distance of about 7 mm or approximately the radius of the disk source. This is illustrated in Figs. 5 and 6.

The curves in Fig. 7 compare again the five-term series result for the same situation as that in Fig. 4 except that the entire volume between the transducer and field points

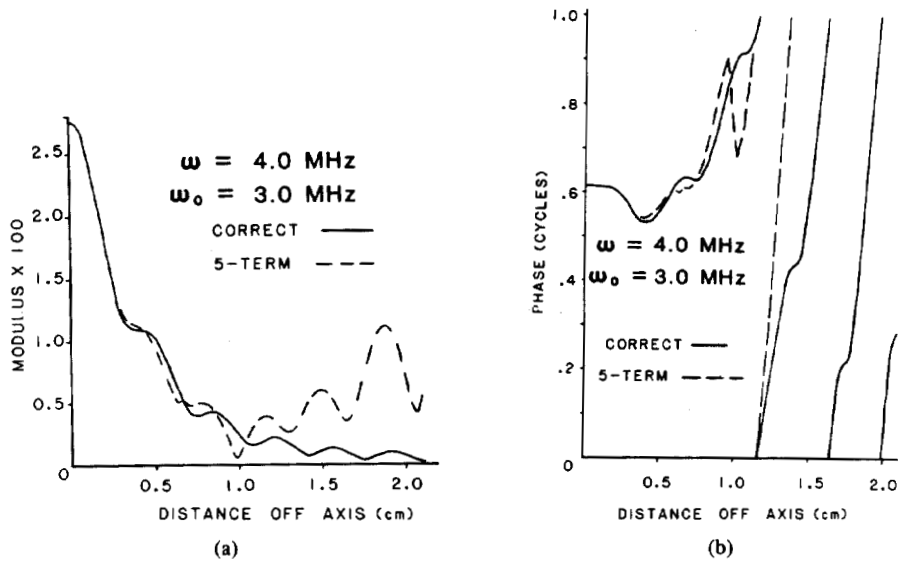


Fig. 6. Five-term Taylor series results (dashed lines) compared with correct results (solid lines) for frequency of 4.0 MHz. All other conditions correspond to those of Fig. 2.

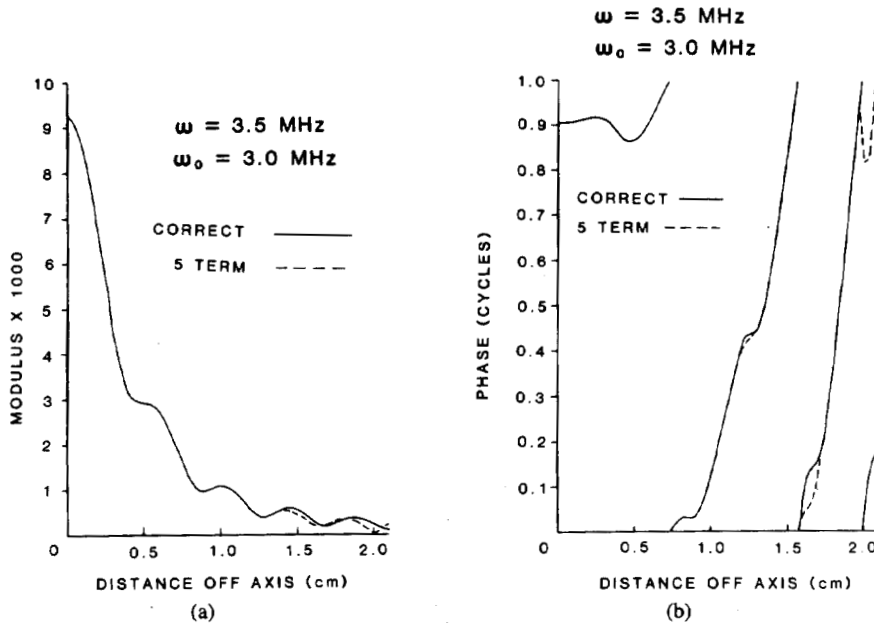


Fig. 7. Five-term Taylor series results (dashed lines) compared with correct results (solid lines) for frequency of 3.5 MHz. All other conditions correspond to those of Fig. 2 except that entire 11 cm region between radiating disk and field points contains attenuating tissue-mimicking material.

contains material with tissuelike attenuation. Again good agreement is demonstrated through the second side lobe.

Finally, to test the five-term series accuracy at a value of y other than 11.0 cm, the results for a frequency of 3.5 MHz and $y = 6.0$ cm are shown in Fig. 8. The entire volume between the transducer and field points contains material with tissuelike attenuation.

IV. COMPUTER TIME SAVINGS

The frequency range required for computation of backscatter coefficients using our method of data reduction [4] for a typical experimental situation using narrow-band

pulses is generally no more than 1 MHz, i.e., $\omega_0 \pm 0.5$ MHz, where the reference frequency ω_0 is the frequency at which the backscatter coefficient is determined. Also, we have found that beam pressures beyond the second side lobe do not contribute significantly. Thus the five-term truncated Taylor series is adequate for use in our determinations of backscatter coefficients.

In the application of our data reduction technique for determining backscatter coefficients, typically $A_{0N}(\vec{r}, \omega)$ is evaluated at 3000 field points \vec{r} and, for each field point, at least 31 frequencies. The time required for these computations via numerical integration using Gaussian

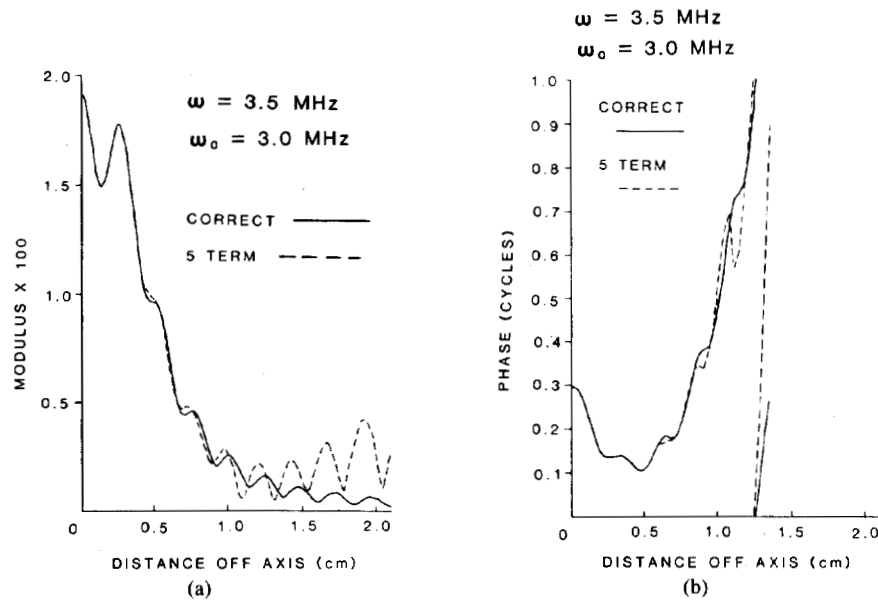


Fig. 8. Five-term Taylor series results (dashed lines) compared with correct results (solid lines) for frequency of 3.5 MHz when axial distance from transducer is 6.0 cm instead of 11.0 cm, and entire region between radiating disk and field points contains attenuating tissue-mimicking material.

quadrature without the Taylor series is 3.4 h using a DEC PDP 11/23+ computer equipped with an array processor. When the five-term Taylor series is used (including computation of the integrals in the coefficients), the time required is about 30 min. Thus the CPU time is reduced to $1/7$. If more than 31 frequencies per field point are desirable, the time savings is greater.

Another advantage of the Taylor series use is that the core memory and input/output time required are greatly reduced when the Taylor series is used. For example, suppose that a recomputation of a backscatter coefficient is needed to assess the effect of uncertainty in the value of the mass density of the scatterers in a tissue-mimicking material. Thus all complex values of $A_{0N}(\vec{r}, \omega)$ involved should be stored for retrieval. Borrowing relevant values from the above example, 3000 field points are involved with 31 complex numbers at each field point corresponding to the 31 frequencies. At 64 bits, or 8 bytes, per single precision complex number, this amounts to 744 kbytes of memory. When the Taylor series expansion is used, it is only necessary to store five complex numbers (coefficients) for each field point instead of 31; thus the memory needed is 120 kbytes instead of 744. The total core memory in our DEC PDP 11/23+ is 512 kbytes, and at least 120 kbytes is available for storage. Therefore, by using the Taylor series we can avoid the need for noncore storage, and input/output time savings can be considerable. Even if the same storage mode is used, the input/output time savings factor is $120/744 \cong 1/6$.

V. SUMMARY AND DISCUSSION

Employment of the five-term (truncated) Taylor series to compute accurate complex pressure fields for 31 fre-

quency values per field point, such as is involved in data reduction to determine backscatter coefficients in our laboratory, results in a reduction of PDP 11/23+ CPU time required to about $1/7$ of that without using the series. Also resulting is a reduction of input/output time by a factor of $1/6$, or better. Estimation of time savings for other applications can be made accordingly.

When the attenuation coefficient is nonzero, causality, via the Kramers-Kronig relations [9], requires that there be some dependence of the ultrasonic speed c on the frequency. In general, the greater the attenuation coefficient and its related dependence on the frequency, the greater the dependence of c on the frequency. In tissues the frequency dependence of the ultrasonic speed is known to be very small, and in the generation of the figures in this work, this dependence has not been introduced. In our treatment, however, almost all of the effect of the frequency dependence of c occurs in the factor e^{-ikr} on the left of (8). In recovering $A_0(\vec{r}, \omega)$ after expanding and evaluating $e^{-ikr} A_0(\vec{r}, \omega)$, the result was multiplied by e^{ikr} in which $c = c(\omega) = c(\omega_0) = \text{constant}$. To account for almost all of the effect of the frequency dependence of c , the real part of k in this recovering factor e^{ikr} could be made $\omega/c(\omega)$ where $c(\omega)$ is the ultrasonic speed as shifted from $c(\omega_0)$ via the Kramers-Kronig relations. The fact that $c = c(\omega_0)$ is used in evaluating the right side of (8) results in a small error because $(r' - r)$ in the integrand is in general small. It is possible, however, that for extreme situations, such as when $\omega - \omega_0$ and $\alpha(\omega)$ are large and r is of the order of the diameter of the radiating element, that the effect of neglecting the frequency dependence of c on the right side of (8) would not be negligible.

In a paper in preparation, work will be reported in which the Taylor series expansion has been applied to focused radiators, and in that paper the Kramer-Kronig relations have been completely represented, resulting in no approximation for causality. Because of the prevalence of focused radiators in the generation of *B*-scan images, this Taylor series expansion will be valuable, not only in backscatter coefficient determination, but in computer modeling of *B*-scan texture patterns [6], [7]. In the case of the texture modeling, we estimate that there will again be a savings in CPU time to generate $A_0(\vec{r}, \omega)$ values by a factor of 1/7. In addition, input/output time savings will correspond to a factor of about 1/8.

REFERENCES

- [1] E. L. Madsen, M. M. Goodsitt, and J. A. Zagzebski, "Continuous waves generated by focused radiators," *J. Acoust. Soc. Amer.*, vol. 70, pp. 1508-1517, 1981.
- [2] H. T. O'Neil, *J. Acoust. Soc. Amer.*, vol. 21, pp. 516-526, 1949.
- [3] J. C. Lockwood and J. G. Willette, *J. Acoust. Soc. Amer.*, vol. 53, pp. 735-741, 1973.
- [4] E. L. Madsen, M. F. Insana, and J. A. Zagzebski, "Method of data reduction for accurate determination of acoustic backscatter coefficients," *J. Acoust. Soc. Amer.*, vol. 76, pp. 913-923, 1984.
- [5] M. F. Insana, E. L. Madsen, T. J. Hall, and J. A. Zagzebski, "Tests of the accuracy of a data reduction method for determination of acoustic backscatter coefficients," *J. Acoust. Soc. Amer.*, vol. 79, pp. 1230-1236, 1986.
- [6] M. F. Goodsitt, E. L. Madsen, and J. A. Zagzebski, "A three dimensional model for generating the texture in B-scan ultrasound images," *Ultrasonic Imaging*, vol. 5, pp. 253-279, 1983.
- [7] J. A. Zagzebski, E. L. Madsen, and M. M. Goodsitt, "Quantitative tests of a three-dimensional gray scale texture model," *Ultrasonic Imaging*, vol. 7, pp. 252-263, 1985.
- [8] M. M. Goodsitt, E. L. Madsen, and J. A. Zagzebski, "Field patterns of pulsed, focused ultrasonic radiators in attenuating and nonattenuating media," *J. Acoust. Soc. Amer.*, vol. 71, pp. 318-329, 1982.
- [9] V. L. Ginsberg, "Concerning the general relationship between absorption and dispersion of sound waves," *Soviet Phys. Acoust.*, vol. 1, pp. 32-41, 1955.



Ernest L. Madsen received the B.S. and the M.S. degrees in physics from the University of Maryland, College Park, and the Ph.D. degree in physics from the Catholic University of America, Washington, DC.

He is an Associate Professor of Medical Physics at the University of Wisconsin, Madison. His research encompasses a range of subjects in medical ultrasound, including imaging, hyperthermia, and biological effects. He also pursues development of test objects for use in medical nuclear

magnetic resonance imaging.



of America.

Timothy J. Hall was born in Flint, MI, in 1956. In 1983 he received the B.S. degree in physics, *summa cum laude*, from the University of Michigan, Flint, and was a Maize and Blue Scholar. He received the M.S. degree in medical physics in 1985 from the University of Wisconsin, Madison, where he is currently working toward a Ph.D., also in medical physics.

His research interests are in ultrasound tissue characterization and medical imaging in general.

Mr. Hall is a member of the Acoustical Society



James A. Zagzebski received the B.S. degree in physics from St. Mary's College, Winona, MN, and the M.S. degree in physics and the Ph.D. degree in radiological sciences from the University of Wisconsin.

He is Professor of Medical Physics and of Radiology and Human Oncology at the University of Wisconsin. His research interests include medical imaging, diagnostic ultrasound, and ultrasound hyperthermia.



Michael F. Insana (M'85) was born in Portsmouth, VA, on December 18, 1954. He received the B.S. degree in physics from Oakland University, Rochester, MI, in 1978, and the M.S. and Ph.D. degrees in medical physics from the University of Wisconsin, Madison in 1982 and 1983, respectively.

He is currently a research physicist at the Center for Devices and Radiological Health, Food and Drug Administration in Rockville, MD. His research interests in medical imaging include ultrasonic and magnetic resonance imaging and tissue characterization, and statistical pattern recognition techniques.

Dr. Insana is an associate member of the Acoustical Society of America.